ChemPhotoChem

Research Article
doi.org/10.1002/cptc.202300177

Chemistry Europe
European Chemical Societies Publishing

www.chemphotochem.org

Comparison of Different Advanced Oxidation Processes (AOPs) and Photocatalysts for the Degradation of Diclofenac

Francesco Conte,[a] Matteo Tommasi,[a] Simge Naz Degerli,[b] Elia Forame,[a] Marco Parolini,[c] Beatrice De Felice,[c] Gianguido Ramis,[d] and Ilenia Rossetti*[a, b]

Diclofenac sodium salt was photodegraded by means of advanced oxidation processes (AOPs), such as Fenton, photo-Fenton and heterogeneous photocatalysis. For the latter different photocatalysts were compared, namely commercial titania P25 and titania metallized with gold (0.1% Au/P25), silver (1% Ag/P25) and palladium (0.1% Pd/P25). Homogeneous treatments demonstrated effective in the degradation of the selected pollutant (>80% conversion @2 h) when the irradiation occurred within the solution. Also, photo-Fenton process assisted by visible light rather than UV was effective but slower and characterized by a toxicity of the residual solution due to unreacted H_2O_2. The photocatalyzed treatment performed at its best when P25 was used (70% conversion @2 h), while modified photocatalysts reached the same conversion when H_2O_2 was added to the solution. Overall, in vitro toxicity tests using Daphnia Magna unveiled that the wastewater treated via M/TiO_2 treatment and photo-Fenton under UV in combination with H_2O_2 showed an acute toxicity comparable with the control group (almost 100% viability @48 h). Conversely, the other processes failed to degrade completely either the pollutant or the hydrogen peroxide, leading to the mortality of 30–80% of the individuals. An important outcome of the work is the direct comparison of different treatments to optimise the outcome, i.e. rapidity of degradation and non toxicity of the treated solution for living bodies.

1. Introduction

Every human activity, from a simple home shower to an industrial treatment, generates directly or through less evident routes huge amount of wastewater which may contain organic molecules, inorganic salts, heavy metals etc..[1] In the last decades, emerging contaminants such as pharmaceuticals and personal care products (PPCPs), pesticides, dyes, antibiotics, antibiotic resistant genes (ARGs) have taken a significant attention.[2] The regulations may vary widely across different regions, nonetheless the wastewater usually needs to be treated before disposing of it in the environment. In most cases, the concentration of the pollutants will be the key parameter to understand whether a treatment may be feasible to carry out and sustainable from an economical point of view. In addition, the wastewater remediation is even more challenging when multiple pollutants are mixed, as each molecule is likely to require a specific treatment in order to lower its concentration below the level suggested by regulations. This is the case of the emerging pollutants, which are compounds whose production began in recent times and their impact on both the environment and human health is still uncertain.[3]

These molecules are freely released in water streams and ultimately may reach the ground water, where they persist for a long time and for many of them a lack of regulations does not allow to prevent release and accumulation in the ecosystem. In addition, a great amount of these compounds belongs to the pharmaceutical sector as wealthy countries tend to consume more drugs, which are metabolized by the liver and excreted in the urine.[4,5] As an example of pharmaceutical most used product which is synthetic, non-steroidal anti-inflammatory medicine called diclofenac, is used for painful, inflammatory disorders of both rheumatic and non-rheumatic origin. It is used extensively in the EU and found in numerous wastewater treatment plants (WWTP), with the concentration range from 0.14 to 1.6 m/L.[6] Along with the direct toxicity of the metabolites towards the aquatic organisms, another concerning side effect is represented by the possible effect of host organisms that come in contact with these molecules, as exemplified by the possible creation of "superbugs", which are bacteria and viruses that become resistant toward certain drugs after a constant exposure to the active principle.[5] Thus,

[a] F. Conte, M. Tommasi, E. Forame, I. Rossetti
Chemical Plants and Industrial Chemistry Group, Dipartimento di Chimica, Università degli Studi di Milano, CNR-SCITEC, via C. Golgi 19, I-20133 Milan, Italy
E-mail: ilenia.rossetti@unimi.it
Homepage: https://sites.unimi.it/Rossetti

[b] S. N. Degerli, I. Rossetti
INSTM Unit Milano-Università, via C. Golgi 19, I-20133 Milan, Italy

[c] M. Parolini, B. De Felice
Dipartimento di Scienze Politiche ed Ambientali, Università degli Studi di Milano, via Celoria 26, I-20133 Milan, Italy

[d] G. Ramis
Dipartimento di Ingegneria Chimica, Civile ed Ambientale, Università degli Studi di Genova and INSTM Unit Genova, via all'Opera Pia 15 A, I-16145 Genoa, Italy

preventing unnecessary releases is very important so treatments that are able to process large amounts of very diluted wastewater that contains various organic molecule, need to be developed, possibly without relying to microorganisms as biological treatment to avoid undesired inurement. Thus various treatment methods have been investigated for the removal of these contaminants from wastewater, such as adsorption technology, chemical oxidation processes, including Fenton oxidation, ozonation, ionizing radiation technology, sulfate radical-based technology, UV/chlorine advanced oxidation. Between those, Advanced Oxidation Processes (AOPs) have a great attention due to its simplicity, efficiency and environmental friendliness.[7,8]

AOPs make possible complete mineralization or total oxidation of pollutants resulting into inorganic products, such as CO_2,H_2O and harmless inorganic compounds.[9] And they have gained additional interest due to the strong oxidation capacity of the hydroxyl radical ($^{\bullet}OH$), with redox potential of 2.8 V.[2,10] The key feature is that they produce *in-situ* an oxidant species or rather a highly reactive molecule which subsequently reacts with the target pollutant, causing its mineralization.[11] In comparison to other AOPs, Fenton/ Fenton-like processes based on the decomposition of H_2O_2 to produce $^{\bullet}OH$ have been chosen due to the simple operation, mild condition and fast formation rate of $^{\bullet}OH$.[12–14] It has been favoured thanks to its great potential to oxidize most organic contaminants to smaller molecular organic compounds and even to mineralize them into CO_2 by the in-situ generated reactive oxygen species (ROS).[7] In details, the active species in the Fenton reaction is the hydroxyl radical, which is generated in a catalytic cycle that involves hydrogen peroxide and ferrous ion, according to (Eq. 1). The latter is regenerated by the same H_2O_2 present in solution (Eq. 2).

$$H_2O_2 + Fe^{2+} \rightarrow OH^- + OH^{\bullet} + Fe^{3+} \quad (1)$$

$$H_2O_2 + Fe^{3+} \rightarrow HO_2^{\bullet} + H^+ + Fe^{2+} \quad (2)$$

$$H_2O_2 + Fe^{3+} + h\nu \rightarrow H_2O^{\bullet} + H^+ + Fe^{2+} \quad (3)$$

$$H_2O_2 + h\nu \rightarrow 2HO^{\bullet} \quad (4)$$

Since reaction (2) is kinetically slow and may limit the overall efficiency of the process, the Photo-Fenton reaction has been developed in order to speed it up (3).[15] Furthermore, depending on the wavelength of the light employed, it may be possible to direct split the hydrogen peroxide into hydroxyl radical (4). In the latter case, it is not necessary any catalyst at all as in case of the UV/H_2O_2 process.[16,17]

Despite the versatility of these treatments, they still require the addition of stoichiometric amount of oxidant and at the end of the process there may be iron sludges that needs to be filtered before the disposal (except in case of H_2O_2/UV process). In order to overcome this limitation, heterogeneous photocatalysis can be adopted, since the photocatalyst can be filtered from the wastewater or (better) used in immobilized form and it does not require the addition of an oxidant, due to the ability of the photoactive material, a semiconductor, to generate the oxidant *in situ* upon irradiation with a proper wavelength.[18] The heterogeneous catalysts have been enhanced from iron-based materials to the materials that are modified or dominated by free-iron multivalent metal,[19] and then to the materials that are doped with oxygen defects or non-metals, such as S, C, N, etc.[19] Photocatalytic activation of O_2 is generally occurring when the photoelectrons from the semiconducting materials are formed under the light irradiation.[20]

When light of energy higher than the semiconductor band gap hits the solid, an electron (e^-) is promoted from the valence band to the conduction band of the photocatalyst. This electron can be used to generate strongly oxidizing hydroperoxyl species reacting with dissolved oxygen. Simultaneously a hole (h^+) is left in the valence band, which can promote oxidation reactions with the substrate adsorbed at the surface.[21,22] However, the efficiency of this process depends on the degree of charge separation and the lifespan of the photogenerated couple,[23] which can be improved by depositing metals with proper work function as electron sinks.

In this paper we have compared different options for the degradation of a model emerging pollutant through Advanced Oxidation Processes. The emerging pollutant that was used in this work is the sodium salt of Diclofenac, which was classified as compound of great concern by the European Union through its JRC (Joint Research Centre) based in Ispra (Italy). Indeed, decision the EU Commission Decision 495/2015, later revised in 2020, introduced a list of compounds whose aquatic concentration have to be closely monitored in order to asses potential risk for the aquatic ecosystem and support future legislation.[24] Among the emerging compounds to be monitored in EU aquatic ecosystems, Diclofenac (DCF) was identified as a high risk substance to be prioritized already in the EU Directive 2013/39/EU and it is one of the 10 substances/groups of substances included in the watch list of EU Commission Decision 495/2015.[25] Diclofenac is an extensively adopted anti-inflammatory which belong to Non-Steroidal Anti-Inflammatory Drug (NSAID) category and its annual *pro-capite* consumption has been assessed between 195 and 940 mg.[26] Figure 1 shows

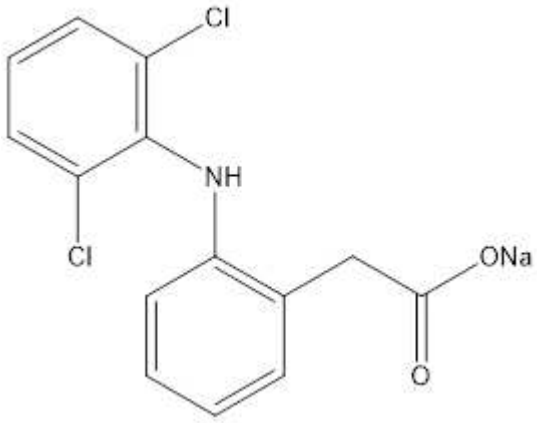

Figure 1. Molecular structure of Diclofenac.

the structure of Diclofenac, which can be summarized as a functionalized di phenyl ammine.

Heterogeneous photocatalysis through titanium dioxide-based materials was employed since TiO_2 is an abundant, inexpensive, non-toxic and fairly stable compound, despite its wide band gap (BG *ca.* 3.2 eV) that allows the adsorption of wavelength in the UV region only.[27] To enhance the visible light response and boost charge dynamics for increasing the performance of the photodegradation rates the TiO_2 can have some modifications, such as heteroatom doping, vacancy engineering, heterostructure fabrication and dye sensitization.[28] TiO_2 commercial nanoparticles were modified through addition of reduced noble metals (*i.e.* Au, Ag, Pd), leading to better charge separation (Schottky barrier creation) and possibly lower band gap. The selected photocatalysts were tested under various light sources, namely UV and visible light. Heterogeneous photocatalysis has been compared with homogeneous Fenton, Photo-Fenton and direct photolysis of DCF with the aid of H_2O_2.

Experimental

Materials preparation

P25 is a commercial titania composed of anatase and rutile, produced by Evonik, former Degussa, and supplied by EIGENMANN & VERONELLI S.p.A. Titania photocatalysts modified with metallic co-catalysts were obtained via wet impregnation and subsequent reduction at high temperature under hydrogen flow. The selected amount of titania and metal precursor were mixed with distilled water in a round-bottom flask. After 2 h of continuous stirring (400 rpm), the homogeneous suspension was evaporated under reduced pressure. Then the collected powder was dried in a conventional static oven. In order to activate the catalyst, the powder was reduced for 3 h in a tubular oven while heating up to 5 °C/min until the final temperature, which depended on the kind of metal employed, and was set based on a Temperature Programmed Reduction run, according to Table 1.

Materials characterization

X-ray diffraction (XRD) was performed with a Philips 3020 instrument using the Cu–Kα radiation with a graphite monochromator on the diffracted beam.

N_2 adsorption and desorption isotherms of samples were measured with a Micromeritics ASAP2020 apparatus. The isotherms were collected at −196 °C for the samples previously outgassed at 150 °C for 4 h. Micropore volume was calculated according to the t-plot method. Brunauer-Emmett-Teller (BET) linearization was used in the range 0.05–0.30 P/P° to calculate the specific surface area (SSA_{BET}). The Barrett-Joyner-Halenda model (BJH) was used to determine the pore-size distribution from the adsorption branch.

Table 1. Catalyst recipes for photocatalysts preparation via wet impregnation.

Metal salt	Metal loading (%mol)	Mass ratio (mg/g_{P25})	Reduction T (°C)
$AgNO_3$ (>99%)	1.0	21.3	150
$AuCl_3$ (>99%)	0.1	3.8	700
$Pd(NO_3)_2 \cdot 2H_2O$ (40% Pd basis)	0.1	3.3	300

Diffuse Reflectance (DR) UV-Vis spectra of samples were recorded on a Shimadzu UV-3600 Plus Cary 500 UV-Vis NIR spectrophotometer in the range of 200–800 nm, using an integrating sphere and $BaSO_4$ as reference standard. The results were processed according to the Kubelka-Munk theory and using the Equation (5) to convert the reflectance spectra into the absorption spectra.[32]

$$F(R_{-}\infty) = (1 - R_{-}\infty)\,2/2R_{\infty}, \quad (5)$$

$(F(R)h\nu)^{1/r}$ (with $r=2$ or $^1/_2$ for direct and indirect band gap) was plotted vs. hν to obtain the band gap of each sample.[33]

Scanning electron microscopy (SEM) was performed using a FE-SEM LEO 1525 ZEISS (Jena, DE) with acceleration potential voltage of 15 keV. Samples were deposited on conductive carbon adhesive tape and analysed without metallisation.

Transmission Electron Micrographs (TEM) were collected by a Philips 208 Transmission Electron Microscope. The samples were prepared by putting one drop of an ethanol dispersion of the catalysts on a copper grid, pre-coated with a Formvar film and dried in air.

Experimental apparatus and procedures

The kind of reactor employed depended on the light source. Indeed, for experiments carried out under visible white light (LED) and under UV light with an external UV lamp (UV-ext), an open top cylindrical glass reactor (reactor A) was adopted to allow an effective top-down irradiation of the solution. The total internal volume of Reactor A was over 2 L, however, it has been filled up with 1 L of pollutant solution for each analysis. Proper mixing was ensured by means of a magnetic stirrer, while the temperature was monitored thanks to a thermocouple immersed in the liquid phase and constant temperature was achieved by recirculating water at room temperature in the reactor jacket. During the tests, the LED lamp was fixed 100 mm over the top of the solution, while the height of the external UV lamp was 250 mm due to its different shape.

A second reactor (reactor B) with a cylindrical and elongated shape was used with and internal (axial) UV lamp (UV-immersion), since the latter can be immersed directly into the solution from the reactor cap. Reactor B was also jacketed with an internal volume equal to 0.350 L, although 0.250 L of solution were employed for the analysis.

Regarding the light sources, they were a square and flat LED lamp (Yonkers, 30 W, 2,700 lumen), an immersed-UV lamp (Jelosil, HG 100 AS, 125 W, 260 W/m^2, 365 nm peak emission) and a square external UV lamp (Jelosil, HG 200 W L, 250 W, 116 W/m^2, 365 nm peak emission). Lamps irradiance have been periodically tested with a photo-radiometer (type delta OHM HD 2102.2) which operates in the UVA region.

A typical test was carried out by adding the selected amount of Diclofenac (purity ≥ 98, Sigma Aldrich), hydrogen peroxide (35% v/v, Sigma Aldrich) and catalyst (titania for heterogeneous photocatalytic tests, or iron sulphate heptahydrate, >99%, Sigma Aldrich for Fenton and Photo-Fenton) to the reactor filled with part of the necessary water. Then the pH was possibly adjusted by addition of concentrated sulphuric acid (98%, Sigma Aldrich) or sodium hydroxide (1 M solution from pellets, 97%, Sigma Aldrich). Subsequently, distilled water was added until the desired volume. After

30 minutes of continuous stirring at 400 rpm, the first liquid sample was withdrawn to measure the initial concentration, and the treatment started after switching on the lamp. The reactor, the lamp and the stirrer were inserted in a box to isolate the setup from the ambient light and to protect operators from UV, as illustrated in Figure 2.

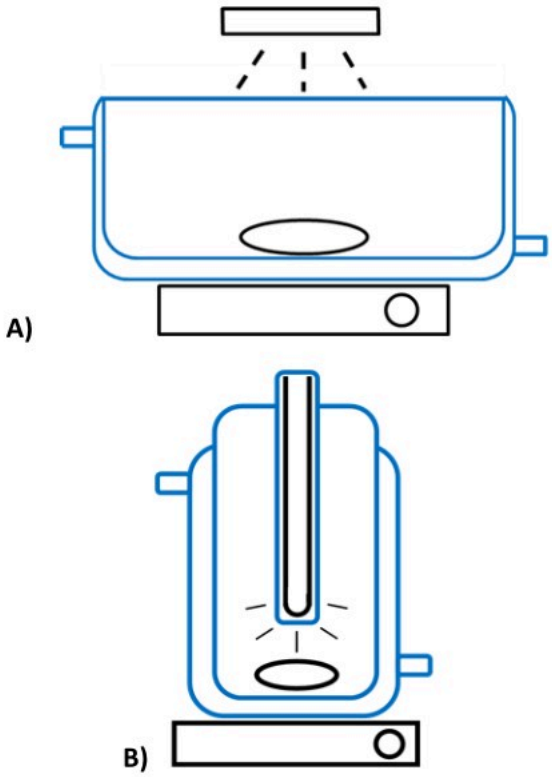

Figure 2. Schematic representation of setup A and setup B employed for carrying out Fenton, Photo-Fenton and heterogeneous photocatalyzed treatments.

The pH vas checked by means of a pH meter (AMEL Instruments, Mod 2335) equipped with a combined glass electrode previously calibrated using two buffer solutions at pH 7 and 4. The conversion achieved by the treatments was monitored at selected reaction times by withdrawing 5 mL of solution, when necessary filtered with cellulose acetate filters (0.20 μm) and analysed by means of a double beam spectrophotometer (Perkin Elmer, Lambda 35). Two quartz cuvette (width 10 mm) were employed, one filled with the sample and the other one filled with the matrix (solution without the pollutant). Results have been in case corrected by taking into account the solution evaporation in the photoreactor, which occurred at the rate of 1 mL per hour of irradiation when the external UV lamp was employed. At the end of the tests the conversion is calculated by using the formula displayed in Equation (6):

$$\%\ Diclofenac\ conversion = \left(\frac{C_0 - C}{C_0}\right)^{*} 100 \quad (6)$$

Acute toxicity tests with Daphnia magna and procedures

Pollutant conversion was monitored by testing the decrease of Diclofenac concentration, but possible partial oxidation intermediates may form, even more toxic than the starting reactant. The final aim of these treatments is to reduce the noxious effect of the pollutant, including its oxidation intermediates, therefore, toxicity tests were performed on the processed solutions using the *Daphnia magna* as model organism. *Daphnia magna* (Figure 3) is a small planktonic cladoceran, the largest in the *Daphnia* genus, with females growing up to 5 mm in size.[29] Because of its peculiar biological and ecological features, *Daphnia magna* is commonly used as model species in diverse research areas, including ecology and ecotoxicology.[30]

The toxicity of the different solutions containing Diclofenac sodium salt alone or their potential by-products generated by different photocatalytic reactions was tested on *Daphnia magna* individuals according to the *Daphnia* sp. Acute Immobilisation Test, OECD 202 guideline.[31]

Daphnia magna individuals came from a single clone obtained from the Istituto Superiore di Sanità (Rome, Italy) and were harvested and maintained in the facility of the University of Milan.

Figure 3. A juvenile (daphnid) of *Daphnia magna*.

Adults were cultured (30 individuals/L) in a commercial mineral water (San Benedetto®) at controlled laboratory conditions.[32] Five replicates containing ten daphnids (i.e., < 24 h-old individuals) each were performed for every experimental condition.

In detail, daphnids were exposed for 48 h at 20 ± 0.5 °C and 16 h light: 8 h dark photoperiod under static, non-renewal conditions in 100 mL of the following solutions: Mineral water (Control), Diclofenac sodium salt (200 ppm), solutions after treatment of Diclofenac sodium salt under UV, UV-TiO_2 (P25), LED-$FeSO_4 + H_2O_2$, UV – 0.1 % Au/TiO_2 (P25) and UV-$FeSO_4 + H_2O_2$ conditions. Viability of individuals was tested after 24 h and 48 h of exposure. Individuals were considered as death when they did not swim for over 15 s, even after a slight agitation of the solutions. Viability of the individuals exposed to the different solutions was compared to that of the control group to assess for acute effects. Acute toxicity tests were replicated twice.

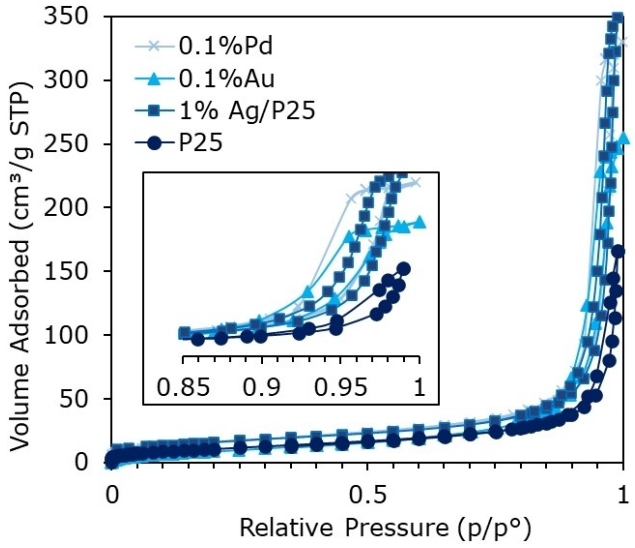

Figure 4. N_2 adsorption/desorption curves of titania photocatalysts.

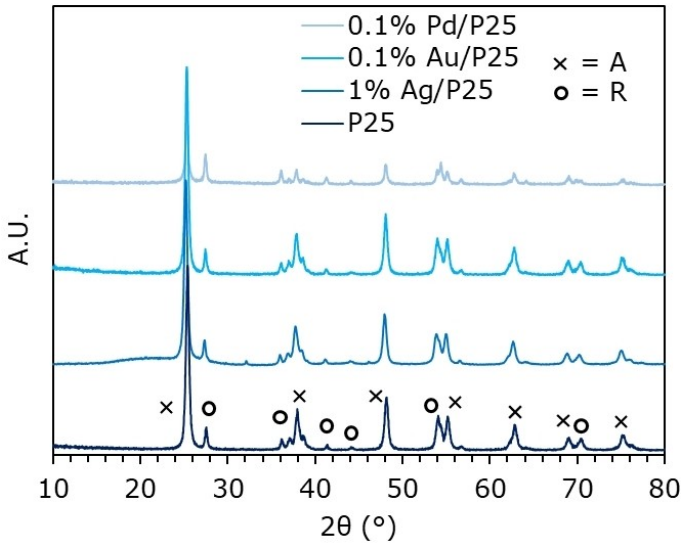

Figure 5. XRD diffraction patterns of photocatalysts. The anatase phase is marked with A, while R stands for rutile.

2. Results and discussion

2.1. Photocatalyst characterization

The BET specific surface area and pore volume were calculated from N_2 adsorption/desorption isotherms (Figure 4 and Table 2). All the samples exhibited type 4 isotherm with poorly pronounced microporous adsorption (at low p/p°) and a small hysteresis of type H3. Generally, the catalysts prepared via reduction at high temperature showed lower surface area, as expected, due to the partial collapse of the pore structure following overheating. The P25 sample was mainly constituted of dense nanoparticles, in which the porosity, if any, was induced by the inter-particle void space.

The XRD patterns are reported in Figure 5 and illustrate that the photocatalysts NPs are crystalline and composed mainly of two titania polymorphs, anatase (*ca.* 74–89 %) and rutile (Table 2). The XRD diffractogram of TiO_2 exhibited the main peaks at 25.28°, 36.93°,48,34°,53.99°,54,93°,62.69°, 68.84°,70.09° and 75.03°,corresponding to (101), (103),(004),200),(105),(211),(204), (113),(220) and (215), while rutile TiO2 at about 27.33°,36,09°, 41.23°, 44.14°, 54.36°, 56.46° could be indexed to (110), (101), (111), (210), (211) and (220), which were in accordance with the standard card (JCPDS no. 21–1276).[33] The addition of the co-catalysts and the following calcination treatment did not change appreciably the proportion between the phases, though a higher loading of Ag (1 % mol/mol) leads to an increased amount of anatase phase. The addition of gold and silver determined a slight increase of the average crystal size, from 15 nm/26 nm (anatase/rutile) up to 19 nm and 28 nm. No different phases relative to the metal co-catalyst were visible, due to the very low loading and high dispersion achieved.

DR-UV-Vis spectra of some representative samples are reported in Figure 6. The data were elaborated in a Tauc Plot, calculating the band gap values reported for every sample in Table 2. The addition of the co-catalysts to P25 decreased in every case the band gap. This feature is attributed to the

Table 2. Catalyst recipes for photocatalysts preparation via wet impregnation.

Sample	BET SSA (m^2/g)	Total pore volume (cm^3/g)	BJH ads. pore width (nm)	Crystallite size (nm)	Phase %	BG (eV)
P25	47	0.257	35	15(A);26(R)	78(A);22(R)	3.40
1 % Ag/P25	56	0.266	36	17(A);15(R)	89(A);11(R)	3.25
0.1 % Au/P25	32	0.394	39	18(A);28(R)	78(A);22(R)	3.14
0.1 % Pd/P25	39	0.511	32	19(A);25(R)	74(A);26(R)	3.14

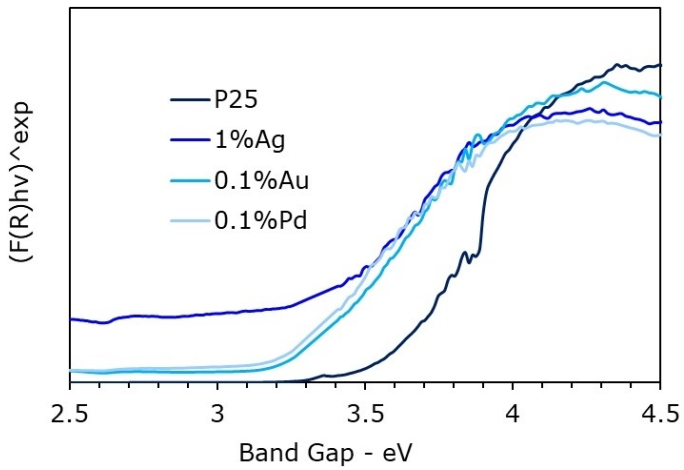

Figure 6. Absorption spectra of selected catalyst and related Tauc Plot.

reduction process at more or less high temperature, which leads to the partial reduction of surface and bulk TiO_2, which is well known to decrease the band gap moving from fully oxidised to black titania. Moreover, it was noticed a small absorption band near 550 nm that is present with the metal-loaded catalysts, and which is attributed to surface plasmon resonance by the metal.

Micrographs from TEM and FE-SEM analyses revealed uniform TiO_2 nanoparticles with very dispersed metals (Figure 7).

2.2. Degradation tests

2.2.1. Blank tests with DCF

The very first attempts have been carried out with reactor A without addition of catalyst and hydrogen peroxide. As expected, under dark conditions or visible light (*i.e.* LEDs) the conversion of a solutions containing 100 ppm of Diclofenac (DCF) was negligible, however, under UV irradiation the solution turned from clear to brown, that is very likely to be a consequence of the direct degradation of the substrate due to exposure to UV radiation (immersion lamp).[34,35] Indeed, the measured absorbance increased up to 20% after 3 h, which sounds counter intuitive for this process if we do not think about the formation of species that absorb more effectively at the selected wavelength.[35–37]

A further test was done with stoichiometric addition of hydrogen peroxide, which is equal to 0.8 mL of 35% H_2O_2 per 100 mg of DCF. The most efficient treatment was the one with immersed UV lamp, resulting in 89% conversion, as illustrated in Figure 8. This result is not surprising, as the visible light cannot directly cleave the oxygen-oxygen bond. Also, the UVA radiation provided by the external lamp was quite ineffective when applied to direct photolysis of DCF.[35] Indeed, measured irradiance of the immersed lamp was two-fold the one of the external lamp (260 W/m^2 vs. 116 W/m^2 respectively).

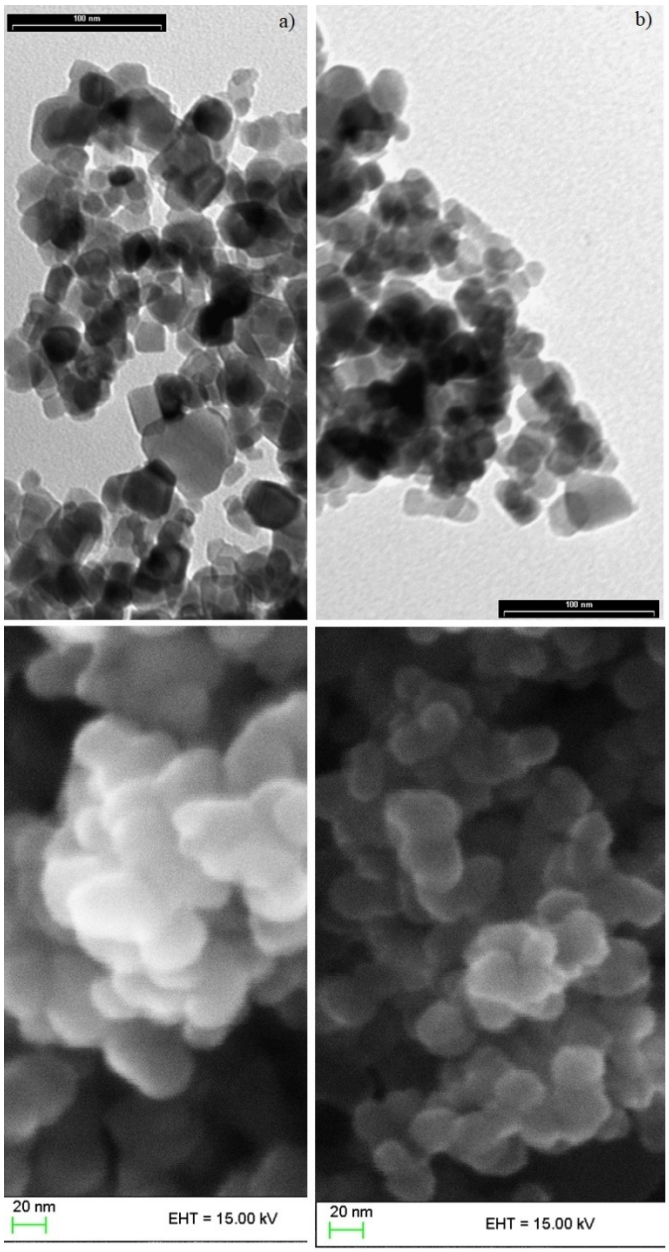

Figure 7. TEM (up) and FE-SEM (down) images of samples 1% Ag/P25 (a) and (b) 0.1% Au/P25.

2.2.2. Photo-Fenton reaction

The Photo-Fenton reaction was carried out first under visible light in order to optimize all the reaction parameters, since a similar setup was adopted successfully during previous investigations with an azo-type dye.[38] First of all, the impact of the pollutant concentration has been investigated on conversion. Four solutions of DCF in the range 12–100 ppm were prepared and tested with reactor A. The initial degradation rate was faster for 50 and 100 ppm solution (Figure 9), due to the higher concentration of pollutant, but higher concentration required longer time to achieve full conversion. The reaction speed in case of diluted DCF (12 ppm) reached a plateau slightly above

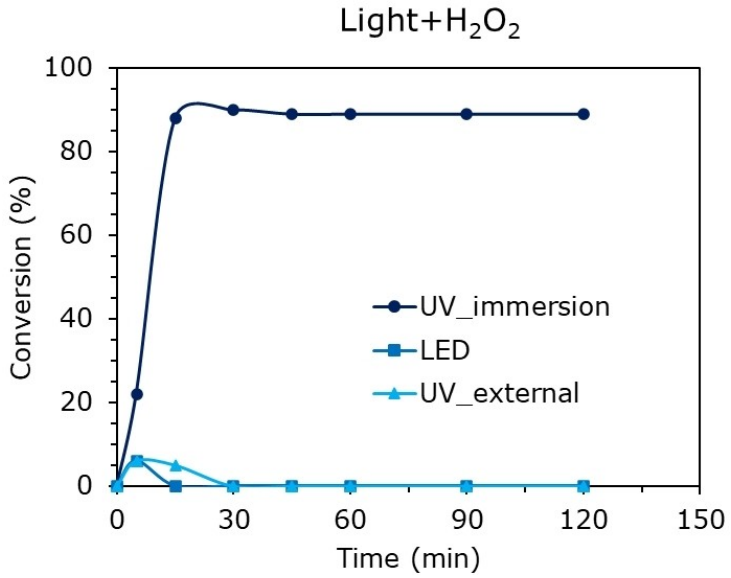

Figure 8. Treatment of a 100 ppm DCF solution, pH 6.5, 1 eq. H_2O_2. Reactor A for LED and external UV lamps, Reactor B for immersed UV lamp.

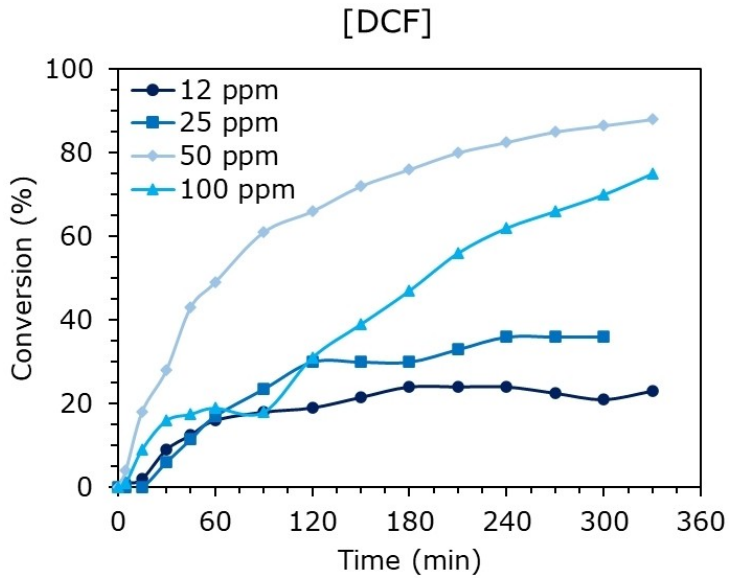

Figure 9. Conversion for Photo-Fenton treatment of various DCF solutions, pH 6.5, 1 eq. H_2O_2, 54 ppm of $FeSO_4$ and visible LED lamp with reactor A.

20% conversion after 3 h, whereas with 25 ppm of pollutant the plateau was reached within 4 h. Overall, it seems that for the photo-Fenton reaction, 50 ppm of DCF represents a good balance between a fast reaction time and a good final conversion, therefore, in all the further tests that concentration of Diclofenac was used. In the literature, different patterns could be observed for this parameter. However, comparable results can be obtained in the study by done Huang.[39] Mineralization efficiency first increased and then decreased with the increase of initial concentration. This phenomenon might associate with the mass transfer limitation between the molecule and reactive oxidation species. High concentration of Diclofenac increased the possibility of collisions between oxidation species and contaminants, which might enhance Diclofenac degradation. However, higher Diclofenac concentration would decrease the mineralization efficiency of Diclofenac since the generated amount of oxidative species are stationary under the constant level of other operational parameters, which could be insufficient to the higher concentration of Diclofenac.[2]

The processes of Fenton/Fenton-like occur at ambient temperature. Reaction temperature has two-side influence of utilization of H_2O_2. Increasing the temperature does not only increase the O_2 diffusion coefficient and facilitates the O_2 reduction, but also enhance the mass transfer of the contaminants.[40] However, higher temperature will decrease the solubility of dissolved O_2 and enhance the self-decomposition rate of H_2O_2 onto H_2O and O_2[2].

Being the DCF a weak electrolyte (pKa 4.15),[41] the effect of the pH on the conversion was also studied. Figure 10 illustrates that the treatment was feasible with similar performance at both pH 3 and native (i.e., 6.5) as over 85% conversion was achieved after 5 h, whereas very poor performance (20% peak conversion) was achieved when operating at pH 12. Anyway, this is a well-known behaviour as the iron salts tend to aggregate into colloids when the pH is increased and these compounds either precipitate or become inactive toward the Photo-Fenton reaction.[42] It is also compatible with the results in the literature.[2] It is observed that low solution pH is desirable for the degradation of the contaminants. However, too low solution pH may not occur the undesired reaction (H_2 evolution reaction) and also has an affect the stability of the heterogeneous catalysts.[43] The optimal pH in Fenton/ Fenton-like process for degradation of organic pollutants is in the range of 2–4. However, in order to reach the optimal pH value for these processes, the addition of chemicals is necessary to adjust the pH, which means increment of operational cost of wastewater treatment. This is also impractical for real wastewaters. To have an efficient removal of contaminants in a broad pH range for the Fenton/Fenton-like processes with in-situ production of H_2O_2 neural pH is desirable.

Since the aim is to obtain a fast and efficient process to diminish the pollutant concentration in wastewater, we tried to decrease the time required to reach higher conversions by varying the iron salt concentration, but this parameter was found not very significant on the performance. Still, working with high concentration of iron can rise concerns about the formation of iron sludges at the end of the treatment, which of course need to be filtered and removed.

Similarly, doubling the amount of hydrogen peroxide did not shorten the reaction time. Indeed, even under UV irradiation with the external lamp a 97% DCF conversion was reached after 4 h.

Vogna et al.[44] reported that the degradation of DCF in a UVC/H_2O_2 system is affected by oxidant concentration only during the late stage of reaction, as Diclofenac is directly cleaved by UV light and then the intermediates are further oxidized by the H_2O_2. In our setup it was used a lamp that emits at longer wavelength, thus, it is likely that the hydrogen peroxide participates in the degradation process since the beginning. In addition, Ledakowicz reported that H_2O_2 in quantity of millimoles and above prevents the radiation from reaching the substrate, as the photons are almost completely absorbed by the oxidant itself, so increasing its concentration does not lead to a greater conversion due to the fixed amount of photons provided by the lamp.[45]

2.2.3. Effect of light source

The kind of setup adopted was found to be very impactful on the overall process performance, as reported in Figure 11. Indeed, it is clearly visible from the graph that the configuration with the external UV lamp outperform the others, as three quarter of the DCF was converted in ca. 1 h. This is not surprising as UV radiation is able to directly cleave hydrogen peroxide as well as help the Fe(III) ion to convert back into the active Fe(II) form. Also, it is interesting to observe that the visible LED lamp was quite effective in boosting the reaction rate, at least in comparison to the Fenton reaction, which was carried out in dark conditions. The former treatment reached 66% conversion after 2 h while the latter achieved 47% conversion in the same time span, then, a plateau was reached in both cases after 5 h, with 80% and 57% conversion, respectively. There are several reasons to prefer visible LEDs

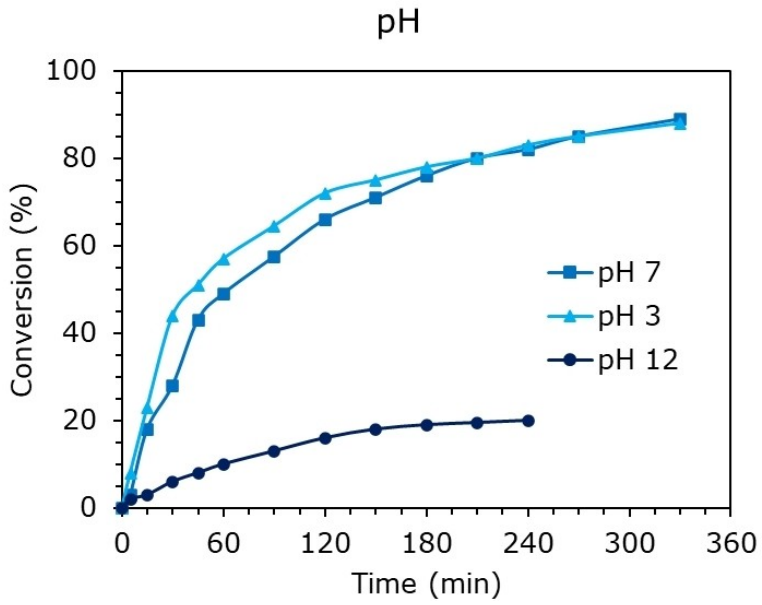

Figure 10. Conversion results for Photo-Fenton treatment of 50 ppm DCF solution, various pH, 1 eq. H_2O_2, 54 ppm of $FeSO_4$ and visible LED lamp with reactor A.

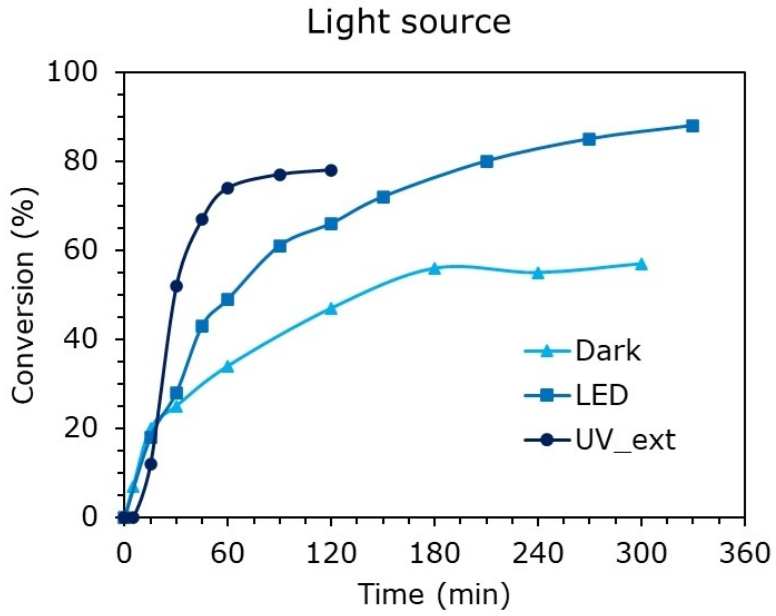

Figure 11. Conversion results through Fenton and Photo-Fenton treatment of 50 ppm DCF solution, pH 6.5, 1 eq. H_2O_2, 54 ppm of $FeSO_4$ and various lamp with reactor A.

over traditional UV lamps, as LEDs are more efficient, release less heat and last longer (over 20,000 h of expected lifespan[46]). In addition, although it depends on the rated power, it is not necessary to protect operators while the lamp is switched on.

2.2.4. Heterogeneous Photocatalysis

The very first tests have been carried out using ca. 200 ppm of titania-based photocatalyst and without the addition of hydrogen peroxide. Indeed, the photocatalyst should be able to generate in-situ the oxidant species through activation of oxygen and hydroxy species through the photogenerated charges. This mechanism works at least under UV irradiation since P25 is not able to absorb significantly visible light, due to its relatively large band gap.[18,47] The prepared P25-based photocatalysts were compared, since these materials have been extensively used by our group for CO_2 photoreduction and photo-reforming, demonstrating particularly active.[48]

Figure 12 illustrates the results of the photocatalytic degradation process. The best material was bare titania P25, which is counterintuitive as the metal-loaded materials showed reduced BG and should be characterised by longer charges lifetime. Moreover, metal-modified P25 samples were active for similar processes, such as glucose photo-reforming to hydrogen.[48]

In details, conversion using pure P25 steadily increased in the first half an hour of treatment, slowing down after 60% conversion until reaching a conversion plateau of 72% at 2 h. On the other hand, 0.1% Au/P25 achieved 34% conversion of DCF within the same time and 47% after 5 h. The worst performers were achieved with 0.1% Pd/P25, with 10% conversion after 5 h, and with 1% Ag/P25.

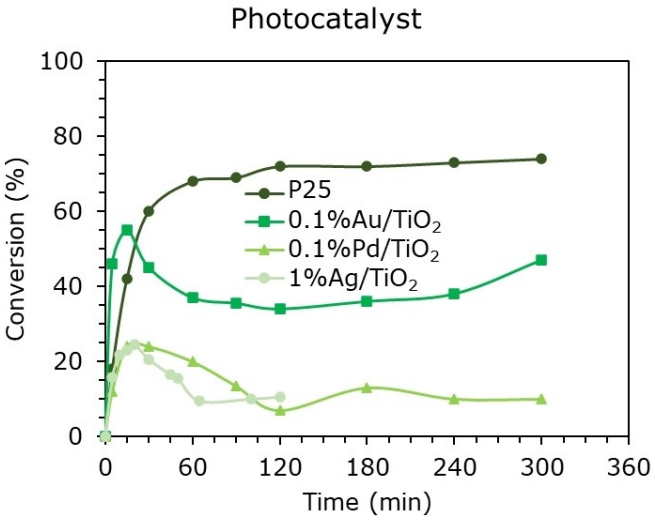

Figure 12. Conversion results with Photo-TiO_2 treatment of 100 ppm DCF solution, external UV lamp, pH 6.5 and 200 ppm of various photocatalysts.

For all the modified photocatalysts, DCF conversion was maximum after ca. 15 minutes of reaction, then it decreased to rise again in the late stage of the process, again probably due to the formation of oxidation intermediates that absorb at the same wavelength of the pollutant and lead to an apparent increase of absorbance rather than a decrease.[35–37]

Kim reported that the photodegradation of organic pollutants was enhanced by the metallization of the titania surface with Pd (and Au to a smaller extent) though a significantly higher loading (ca. 1% wt.) was employed.[49] Two of our samples showed a lower SSA than P25, respectively 32 and 39 m^2/g for 0.1% Pd/P25 and 0.1% Au/P25, and larger crystallite size, while 1% Ag/P25 had a SSA of 56 m^2/g and a quite high

band gap (3.24 eV), though lower than are titania. These modifications are attributed mainly to the thermal reduction step, therefore, our preparation technique may not be suitable to obtain photoactive materials with a high activity in the photodegradation of pollutants, while alternative approaches such as photo-deposition might be more appropriate since a reduction step at high temperature is not required.[49,50] 1% Ag/P25 was prepared at low temperature (around 150 °C) and by increasing the loading of the metal, but its porosity was low if compared to 0.1% Au and 0.1% Pd samples.

Overall, co-catalysts addition is usually done to enhance the lifetime of photogenerated charges. If this is not the rate limiting step, negligible or detrimental effect can be achieved. One possible reason is the surface obscuration by the deposed metal, not expected here due to limited metal loading. Another reason can be the injection of hot electrons by plasmonic metals that enhance the reductive character of the semiconductor instead of the oxidative one.

To improve the conversion, we combined the photocatalyst in form of powder with H_2O_2. It is worth to underline that despite the addition of a sacrificial oxidant, this setup still has some advantages over the Photo-Fenton reaction as the photocatalyst can be separated more easily at the end of the process than the iron sludge. Figure 13 illustrates that the initial reaction rate is high and similar between the materials used in the tests, but the Pd deposited photocatalyst showed again poor performance and a conversion plateau below 35%. Photocatalysts modified with Au and Ag behave similarly, reaching a final conversion of *ca.* 90% after 3 h. Bare titania P25 showed also a short induction time at the beginning of the treatment (5 min), then it catched up with the other deposited materials. Titania modified with silver should be slightly less active than the same material deposited with gold according to the literature,[49] though the present data show about the same performance of Ag at a cost significantly lower than gold.

Further tests were performed to compare the conversion of the Photocatalytic treatment with TiO_2 when the irradiation occurs through different sources. The tests were carried out without the addition of the oxidant and using P25 as benchmark. In details, the two setups were the reactor A with external UV lamp and reactor B with immersed UV lamp. Despite the setups were not directly comparable since the volume of the solutions are different, the distribution of the light changes and so does the lamp rated power, the results reported in Figure 14 show that higher conversion can be achieved with the immersed UV lamp, due to higher irradiance and more effective and uniform dispersion of the photons inside the solution.

Lastly, the effect of photocatalyst concentration on the DCF conversion was investigated, resulting in a slight impact on the

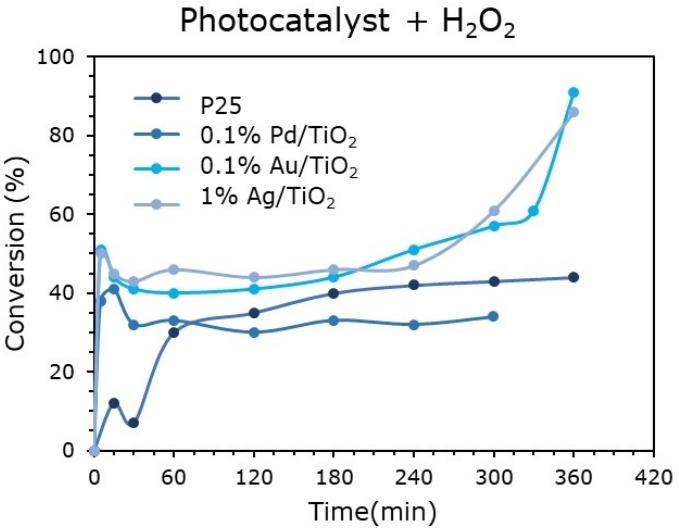

Figure 13. Conversion results with Photo-TiO_2 treatment of 100 ppm DCF solution, external UV lamp, pH 6.5 and 200 ppm of various photocatalysts and 1 eq. of H_2O_2.

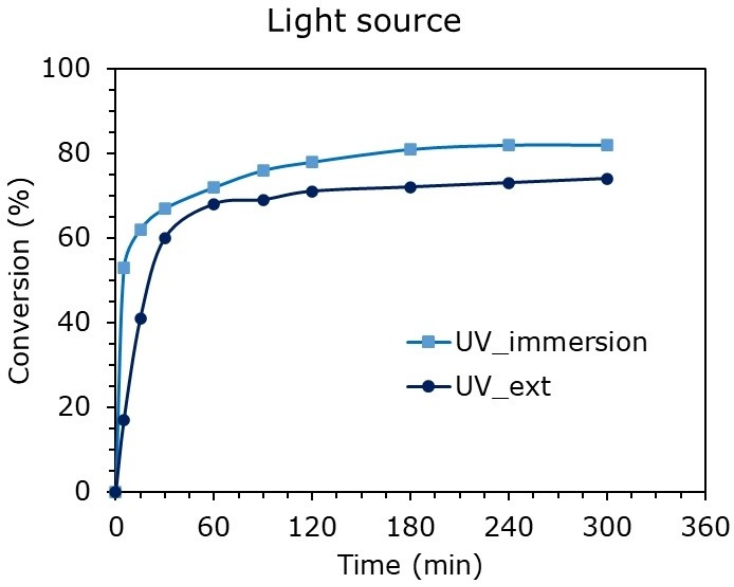

Figure 14. Conversion results after Photo-TiO_2 treatment of 100 ppm DCF solution, external or immersed UV lamp, pH 6.5 and 200 ppm of P25.

treatment. This was not expected as it may be associated with a direct formation of oxidant species and degradation product due to the presence of UV radiation rather than the photo-catalyst itself. Razzaq and co-authors reported a 75% increase in the antimicrobial activity when the concentration of titania increased by a factor of ten,[51] thus, it is likely that our variation is too small to determine an effect on the conversion of pollutant. In addition, increasing the amount of photocatalyst by that extent may not be economically feasible from an industrial point of view.

2.2.5. Comparison of different treatments

A final comparison is made to understand which treatment was the most effective (Figure 15). Treatments that employ UV lamps reached higher conversion within the first minutes of reaction, as in case of Photo-TiO_2 with 0.1% Au/P25 and P25. Moreover, the same graph confirms that the immersed lamp was more efficient than the external one in delivering irradiation to the solution with an overall higher and better dispersed irradiance, although the first setup is less likely to be adopted on a large scale as it requires expensive lamps and pipes with housing for the illumination system. Despite a slower reaction rate at the beginning, the Photo-Fenton process with LEDs eventually reached a DCF conversion of 70%, which sits between the one of P25 (82%) and 0.1% Au/P25 (58%). Overall, is quite an impressive result since a much more convenient irradiation system can be successfully employed at the expenses of increasing the reaction time. Similar conclusion was achieved in a previous work on the degradation of azo-dyes, so this treatment may be a good candidate for degrading a broad spectrum of organic compounds. This comparison can allow the selection of the best treatment method for a given pollutant.

2.3. Toxicity tests

The conversion performance alone does not assess if the treatment is effective in reducing the toxicity of the wastewater as the leftover pollutant can still be noxious and incomplete degradation may even lead to more harmful compounds. Thus, in order to estimate the validity of each treatment, the most interesting samples were tested for acute toxicity using *Daphnia magna* (Figure 16). The treatments have been carried out using an increased amount of Diclofenac (i.e. 200 ppm) and 1 equivalent of H_2O_2 in order to allow the preparation of several diluted solutions and to assess their toxicity. In addition, the reaction time was increased to 24 h to completely degrade any residue of oxidant, which would have killed any crustaceous regardless of the DCF concentration,[52] and the distilled water was replaced by commercial San Benedetto water, which is the culture medium in which *Daphnia magna* is bred. All the tests were carried out using the setup A and the photo-catalyst/iron sludges were filtered after the treatment.

The exposure to DCF alone (200 ppm) induced the complete mortality of daphnids after 48 h of exposure (Figure 16). These results agreed previous studies performed on the same biological model, reporting that the effect concentration for the 50% of individuals (EC_{50}) of DCF ranged between 9 e 123 mg/L.[53–58] Our companion study estimated that the EC_{50} of the DCF sodium salt used in this experiment was 78.42 ± 5.21 mg/L (95% confidence intervals = 72.10–84.50).

The results of the acute toxicity tests suggested that some of the photocatalytic treatments were highly efficient in degrading DCF and reducing its toxicity.

Although Photo-Fenton reaction with visible LED light might be successful in the mineralization of DCF, the visible light was not able to degrade H_2O_2, resulting in a complete mortality of daphnids at the end of the exposure.

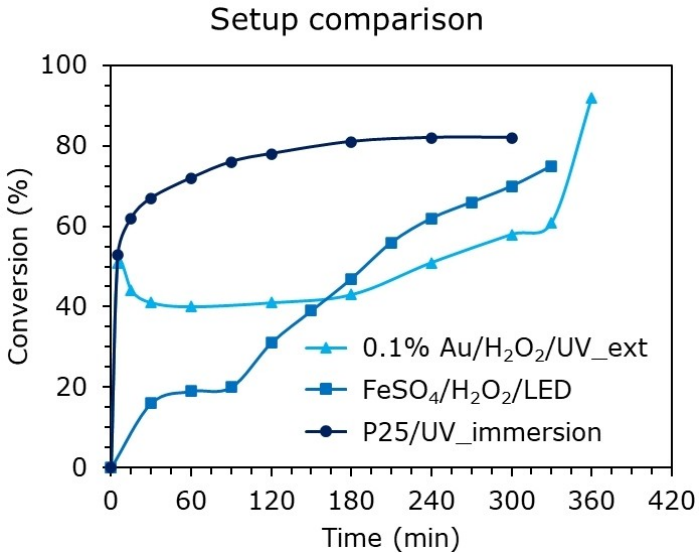

Figure 15. Conversion results of various photocatalyzed treatment. 50 ppm DCF solution, pH 6.5 and 1 eq of H_2O_2 (Photo-TiO_2 and Photo-Fenton), 54 ppm $FeSO_4$ (Photo-Fenton).

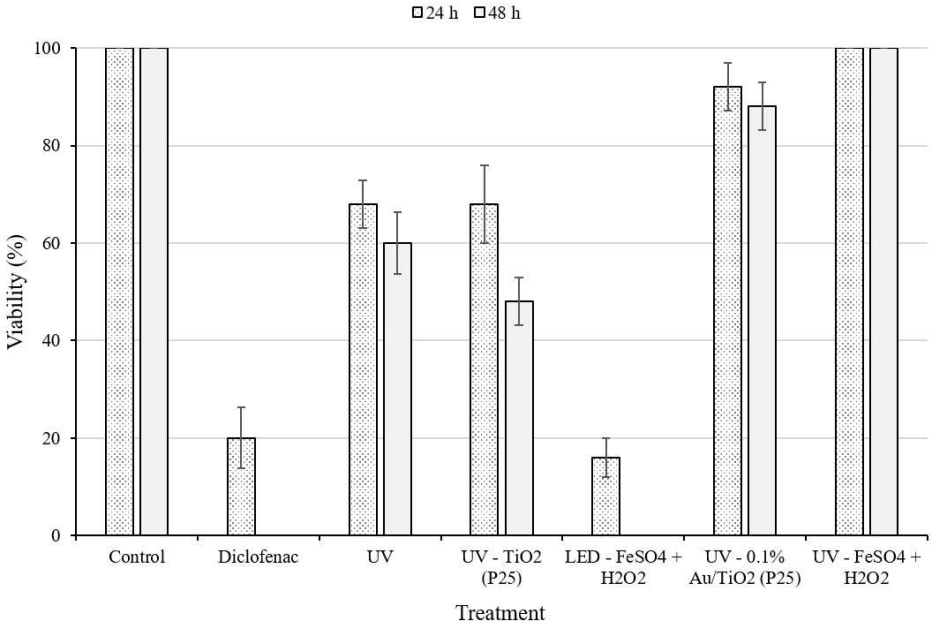

Figure 16. Percentage of survival of *Daphnia magna* individuals after the 48 h exposure to solutions deriving from different photocatalytic treatments for removing DCF from the water.

The exposure to solutions from photolysis of DCF with UV light alone returned a mortality up to the 40% of individuals.

Photolysis of DCF with UV light left the viability of the daphnids to 70% after one day and 60% after two days of exposure to the solution. In that case, a shift in the colour of the solution was observed, from clear to brown, that can be supposed being due to the formation of by-products that could affect viability of daphnids.

Similar results were achieved using photocatalyzed treatment with P25 and under UV light, where a decrease in viability as low as 50% after 48 h was noted. In contrast, the highest survival of daphnids was obtained at the end of the experiments with the solutions from 0.1% Au/P25 under UV light (*ca.* 90% @48 h) and Photo-Fenton under UV (100% @48 h).

On the other hand, also the Photo-Fenton treatment proved to be effective, though the formation of iron sludges is still an issue to be addressed.

3. Conclusions

In this work, several setups of advanced oxidation processes and photocatalysis have been tested and compared. Regarding homogeneous processes, it was observed that photo-Fenton carried out under visible light (LED lamp) was slower than the same treatment under external UV irradiation. A balance is therefore needed comparing the advantages of a LED visible irradiation with those of a more compact apparatus or shorter treatment with UV irradiation.

Using the external lamp, the differences between the bare P25 and surface-modified photocatalysts were highlighted. All the modified photocatalysts (Au, Pd and Ag) performed worse than the benchmark P25 for short reaction times. The addition of an external oxidant (H_2O_2) was found to improve the results and to align the activity of 0.1% Au, 0.1% Pd and 1% Ag with that of bare titania P25.

In the selected conditions the photoreactor with immersed UV lamp in combination with P25 demonstrated to be clearly superior to other arrangements of the lamp since it was possible to degrade the Diclofenac up to 80% in less than 3 h. However, toxicity tests using *Daphnia magna* as model species unveiled that in the latter condition 30% to 40% mortality occurred, probably as a consequence of residual TiO_2.

This change when 0.1% Au/TiO_2 (P25) is used instead of bare P25 under UV light. This type of treatment is able to reduce the toxicity of the solution leading to just a 10% mortality after 24 h of the *Daphnie* used for the test.

Similar results were achieved using the homogeneous photo-Fenton process which leads to a non-toxic solution after it is performed. This is very promising results and looking in a perspective of scale up, even if this type of treatment is slightly slower that other processes, it can represent a suitable technology for the degradation of diclofenac and other drugs.

Acknowledgements

M. Parolini and I. Rossetti gratefully acknowledge Università degli Studi di Milano for support through the grant PSR 2021 – GSA – Linea 6 "One Health Action Hub: University Task Force for the resilience of territorial ecosystems". Alessandro Di Michele from the University of Perugia is gratefully acknowledged for providing FE-SEM and TEM images.

Conflict of Interests

The authors declare no conflict of interest.

Data Availability Statement

All the data are reported in the text

Keywords: Wastewater treatment · Diclofenac · Fenton · Photo-Fenton · AOPs · Photocatalysis · Titanium Dioxide · Daphnia magna

[1] P. Bautista, A. F. Mohedano, J. A. Casas, J. A. Zazo, J. J. Rodriguez, *J. Chem. Technol. Biotechnol.* **2008**, *83*, 1323–1338.
[2] Y. Liu, Y. Zhao, J. Wang, *J. Hazard. Mater.* **2021**, *404*, 124191.
[3] T. Deblonde, C. Cossu-Leguille, P. Hartemann, *Int. J. Hyg. Environ. Health* **2011**, *214*, 442–448.
[4] A. Kulo, M. Y. Peeters, K. Allegaert, A. Smits, J. de Hoon, R. Verbesselt, L. Lewi, M. van de Velde, C. A. J. Knibbe, *Br. J. Clin. Pharmacol.* **2013**, *75*, 850–860.
[5] A. P. Magiorakos, A. Srinivasan, R. B. Carey, Y. Carmeli, M. E. Falagas, C. G. Giske, S. Harbarth, J. F. Hindler, G. Kahlmeter, B. Olsson-Liljequist, D. L. Paterson, L. B. Rice, J. Stelling, M. J. Struelens, A. Vatopoulos, J. T. Weber, D. L. Monnet, *Clin. Microbiol. Infect.* **2012**, *18*, 268–281.
[6] V. T. Tra, V. T. Pham, T.-D. Tran, T. H. Tran, T. K. Tran, T. P. T. Nguyen, V. T. Nguyen, T.-V.-H. Dao, P.-Y.-N. Tran, V.-G. Le, C.-S. Tran, *Case Stud. Chem. Environ. Eng.* **2023**, *8*, 100506.
[7] Y. Liu, J. Wang, *Chem. Eng. J.* **2023**, *466*, 143147.
[8] D. Ghime, P. Ghosh, in *Advanced Oxidation Processes - Applications, Trends, and Prospects*, IntechOpen, **2020**.
[9] P. Kumari, A. Kumar, *Res. Surf. Interfaces* **2023**, *11*, 100122.
[10] J. Shi, J. Jiang, Q. Chen, L. Wang, K. Nian, T. Long, *Arab. J. Chem.* **2023**, *16*, 104856.
[11] D. B. Miklos, C. Remy, M. Jekel, K. G. Linden, J. E. Drewes, U. Hübner, *Water Res.* **2018**, *139*, 118–131.
[12] M. Cheng, C. Lai, Y. Liu, G. Zeng, D. Huang, C. Zhang, L. Qin, L. Hu, C. Zhou, W. Xiong, *Coord. Chem. Rev.* **2018**, *368*, 80–92.
[13] F. Haber, R. Willstätter, *Ber. Dtsch. Chem. Ges. A* **1931**, *64*, 2844–2856.
[14] H. J. H. Fenton, *J. Chem. Soc. Trans.* **1894**, *65*, 899–910.
[15] S. M. Kim, A. Vogelpohl, *Chem. Eng. Technol.* **1998**, *21*, 187–191.
[16] H. Kawaguchi, *Chemosphere* **1992**, *24*, 1707–1712.
[17] G. V. Buxton, C. L. Greenstock, W. P. Helman, A. B. Ross, *J. Phys. Chem. Ref. Data* **1988**, *17*, 513–886.
[18] Y. Nosaka, A. Nosaka, *ACS Energy Lett.* **2016**, *1*, 356–359.
[19] X. Yang, C. Lai, L. Li, M. Cheng, S. Liu, H. Yi, M. Zhang, Y. Fu, F. Xu, H. Yan, X. Liu, B. Li, *Sep. Purif. Technol.* **2022**, *287*, 120517.
[20] Z. Jiang, L. Wang, J. Lei, Y. Liu, J. Zhang, *Appl. Catal. B* **2019**, *241*, 367–374.
[21] V. Etacheri, C. Di Valentin, J. Schneider, D. Bahnemann, S. C. Pillai, *J. Photochem. Photobiol. C* **2015**, *25*, 1–29.
[22] M. A. Fox, M. T. Dulay, *Chem. Rev.* **1993**, *93*, 341–357.
[23] T. Tachikawa, M. Fujitsuka, T. Majima, *J. Phys. Chem. C* **2007**, *111*, 5259–5275.
[24] https://eur-lex.europa.eu/legal-content/EN/TXT/?uri=uriserv%3AOJ.L_.2015.078.01.0040.01.ENG.
[25] M. O. Barbosa, N. F. F. Moreira, A. R. Ribeiro, M. F. R. Pereira, A. M. T. Silva, *Water Res.* **2016**, *94*, 257–279.
[26] L. Lonappan, S. K. Brar, R. K. Das, M. Verma, R. Y. Surampalli, *Environ. Int.* **2016**, *96*, 127–138.
[27] A. Pattnaik, J. N. Sahu, A. K. Poonia, P. Ghosh, *Chem. Eng. Res. Des.* **2023**, *190*, 667–686.
[28] J. Zhang, H. Wu, L. Shi, Z. Wu, S. Zhang, S. Wang, H. Sun, *Sep. Purif. Technol.* **2024**, *329*, 125225.
[29] J. A. H. Benzie, *Cladocera: The genus Daphnia (including Daphniopsis). Guide to the identification of the microinvertebrates of the continental waters of the world*, **2005**, Kenobi Productions, Backhuys Publishers.
[30] B.-Y. Lee, B.-S. Choi, M.-S. Kim, J. C. Park, C.-B. Jeong, J. Han, J.-S. Lee, *Aquat. Toxicol.* **2019**, *210*, 69–84.
[31] OECD, *OECD Guidel. Test. Chem. Sect. 2, OECD Publ. Paris*,, DOI:doi.org/10.1787/9789264069947-en.
[32] B. De Felice, V. Sabatini, S. Antenucci, G. Gattoni, N. Santo, R. Bacchetta, M. A. Ortenzi, M. Parolini, *Chemosphere* **2019**, *231*, 423–431.
[33] K. Wang, Y. Zhuo, J. Chen, D. Gao, Y. Ren, C. Wang, Z. Qi, *RSC Adv.* **2020**, *10*, 43592–43598.
[34] L. Zhang, Y. Liu, Y. Fu, *RSC Adv.* **2020**, *10*, 9907–9916.
[35] M. Kovacic, D. Juretic Perisic, M. Biosic, H. Kusic, S. Babic, A. Loncaric Bozic, *Environ. Sci. Pollut. Res. Int.* **2016**, *23*, 14908–14917.
[36] M. Jiménez-Salcedo, M. Monge, M. T. Tena, *J. Environ. Chem. Eng.* **2021**, *9*, 105827.
[37] P. Iovino, S. Chianese, S. Canzano, M. Prisciandaro, D. Musmarra, *Desalin. Water Treat.* **2017**, *61*, 293–297.
[38] F. Conte, C. Calloni, A. Tripodi, M. Parolini, B. De Felice, G. Ramis, I. Rossetti, *Appl. Catal. B.*
[39] B. Huang, C. Qi, Z. Yang, Q. Guo, W. Chen, G. Zeng, C. Lei, *J. Catal.* **2017**, *352*, 337–350.
[40] J. Tang, J. Wang, *Chem. Eng. J.* **2018**, *351*, 1085–1094.
[41] A. Avdeef, C. M. Berger, C. Brownell, *Pharm Res* **2000**, *17*, 85–89, https://doi.org/10.1023/A:1007526826979.
[42] K. O'Dowd, S. C. Pillai, *J. Environ. Chem. Eng.* **2020**, *8*, 104063.
[43] W. Zhou, X. Meng, J. Gao, A. N. Alshawabkeh, *Chemosphere* **2019**, *225*, 588–607.
[44] D. Vogna, R. Marotta, A. Napolitano, R. Andreozzi, M. D'Ischia, *Water Res.* **2004**, *38*, 414–422.
[45] S. Ledakowicz, E. Drozdek, T. Boruta, M. Foszpańczyk, M. Olak-Kucharczyk, R. Zyłła, M. Gmurek, *Int. J. Photoenergy* **2019**, *2019*, 1–11.
[46] J. Casamayor, D. Su, M. Sarshar, *Archit. Eng. Des. Manag.* **2015**, *11*, 105–122.
[47] A. M. Abdullah, M. Gracia-Pinilla, S. C. Pillai, K. O'Shea, *Molecules* **2019**, *24*, 2147.
[48] F. Conte, I. Rossetti, G. Ramis, C. Vaulot, S. Hajjar-garreau, S. Bennici, *Materials (Basel)* **2022**, *15*(8), 2915 DOI: 10.3390/ma15082915.
[49] J. Kim, D. Monllor-Satoca, W. Choi, *Energy Environ. Sci.* **2012**, *5*, 7647–7656.
[50] H. Dong, G. Zeng, L. Tang, C. Fan, C. Zhang, X. He, Y. He, *Water Res.* **2015**, *79*, 128–146.
[51] Z. Razzaq, A. Khalid, P. Ahmad, M. Farooq, M. U. Khandaker, A. A. M. Sulieman, I. U. Rehman, S. Shakeel, A. Khan, *Catalysts* **2021**, *11*, 709.
[52] E. S. Reichwaldt, L. Zheng, D. J. Barrington, A. Ghadouani, *J. Environ. Eng. (United States)* **2012**, *138*, 607–611.
[53] B. Ferrari, N. Paxéus, R. Lo Giudice, A. Pollio, J. Garric, *Ecotoxicol. Environ. Saf.* **2003**, *55*, 359–370.
[54] M. Cleuvers, *Ecotoxicol. Environ. Saf.* **2004**, *59*, 309–315.
[55] H. H. Guk, G. H. Hor, D. K. Sang, *Environ. Toxicol. Chem.* **2006**, *25*, 265–271.
[56] T. Haap, R. Triebskorn, H. R. Köhler, *Chemosphere* **2008**, *73*, 353–359.
[57] J. Lee, K. Ji, Y. Lim Kho, P. Kim, K. Choi, *Ecotoxicol. Environ. Saf.* **2011**, *74*, 1216–1225.
[58] J. Drzymała, J. Kalka, *Chemosphere* **2020**, *259*, 127407.

Manuscript received: August 7, 2023
Revised manuscript received: October 30, 2023
Accepted manuscript online: December 11, 2023
Version of record online: ■■, ■■

RESEARCH ARTICLE

Different advanced oxidation processes (AOPs), such as Fenton, photo-Fenton and heterogeneous photocatalysis have been tested towards the degradation of Diclofenac sodium salt. Toxicity tests performed using *Daphnia magna* as model species unveiled the type of treatment which allows detoxification of the solution.

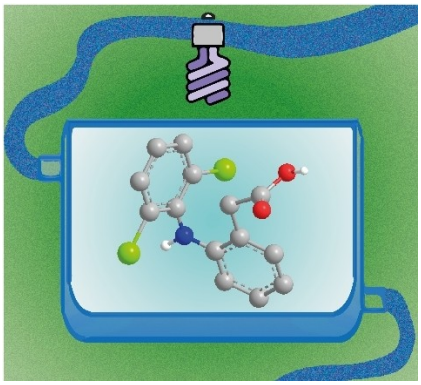

*F. Conte, M. Tommasi, S. N. Degerli, E. Forame, M. Parolini, B. De Felice, G. Ramis, I. Rossetti**